Natural Resources Research, Vol. 30, No. 1, February 2021 (© 2020)
https://doi.org/10.1007/s11053-020-09720-5

Original Paper

Natural Attenuation of Acid Mine Drainage by Various Rocks in the Witbank, Ermelo and Highveld Coalfields, South Africa

E. Sakala,[1,2] F. Fourie,[2] M. Gomo,[2] and G. Madzivire[1,3,4]

Received 10 March 2020; accepted 29 June 2020
Published online: 9 July 2020

In the Karoo coalfields, mining operations that release acid mine drainage (AMD) are threatening groundwater resources. An important parameter controlling the extent and severity of AMD impact is the natural attenuation of rocks in response to AMD. Very little is known about such response of Karoo rocks in saturated and unsaturated conditions, a research gap filled by this paper. Laboratory column leach experiments were used to study the responses of different rock types from the Witbank, Ermelo and Highveld coalfields of South Africa. The results of the experiments show that rock samples with high quartz mineral content offered little attenuation of AMD and those consisting of plagioclase and clays offered some attenuation, while those with high carbonate mineral content, neutralized and reduced the concentration of heavy metals from AMD. The presence of oxygen increased the rate of heavy metal removal from AMD. For all rock samples under saturated and unsaturated conditions, the sulfate and chloride concentrations of AMD remained unchanged after the leaching process, showing that these parameters are conservative and can be used as potential natural tracers of AMD movement in the subsurface. The research shows that laboratory leach tests may be used to rank the various rock types in the Karoo coalfields in terms of their capacity to buffer the impacts of AMD. Such a ranking could inform policy and decision makers in regard to handling and storage of AMD-generating wastes, as well as to location and design of AMD waste storage facilities.

KEY WORDS: Acid mine drainage, Column leach, Coalfield, Saturated, Unsaturated zone, Pollution.

INTRODUCTION

Globally, groundwater is an important and valuable water resource (Hadžić et al. 2015) for various purposes (consumption, irrigation, industry and mining) owing to its relatively low susceptibility to pollution and its abundance. However, groundwater resources are under serious threat by human activities (e.g., mining, industrial, agricultural and waste disposal) which introduce pollutants onto the surface or into the subsurface.

About 85% of South African energy comes from burning of coal from the Mpumalanga Province. As much as coal in South African is major contributor to the energy dynamics, mining of coal is major threat to the groundwater resources in the area. This is because coal in the Mpumalanga Province and its host rock contain pyrite. Iron sulfide,

[1]Council for Geoscience, Pretoria, South Africa.
[2]Institute for Groundwater Studies, University of the Free State, Bloemfontein, South Africa.
[3]Department of Environmental Science, University of South Africa, 28 Pioneer Avenue, Florida Park, Roodepoort 1709, South Africa.
[4]To whom correspondence should be addressed; e-mail: gmadzivire@geoscience.org.za

found in coal host rocks and coal discard dumps, reacts with water in the presence of oxygen to produce acid mine drainage (AMD) which is typically characterized by high sulfate concentrations, pH values less than 7 and elevated concentrations of remobilized metals such as iron, aluminum, manganese and others (Bell et al. 2002; Lapakko 2002; Sakala et al. 2017). The prerequisites for AMD formation are (a) the generation of protons at a faster rate than they can be neutralized by alkaline materials (e.g., carbonates) in the orebody or waste disposal facility, (b) access to oxygen and water and (c) presence of certain bacteria.

The fate of groundwater with regard to AMD generated by mining operations in a typical coalfield is determined by several factors, such as the type of mining operation (opencast or underground), the degree of flooding, the management of mining discards and the transport-attenuation properties of the surface and subsurface. Research to understand how AMD reacts chemically with the various rocks found in a typical coalfield is important to facilitate a regional assessment of the fate of groundwater in a coalfield and to inform policy and decision makers for environmental management purposes. Such research can be done using various field and laboratory tests, including field-scale tests, batch reactor tests, column leach tests and humidity cell tests (Usher et al. 2003; Gautama and Kusuma 2008; Costin et al. 2011; De Souza and Mansur 2011). None of these methods is considered superior to the others, because the choice of method depends on the problem to be solved. In an AMD environment, these tests are done to simulate geochemical weathering processes, to classify hazardous waste, to evaluate acid generation and to predict the quality of drainage from a waste disposal facility (U.S Environmental Protection Agency 1994).

Because column leach tests allow for the simulation of the leaching processes under both saturated and unsaturated conditions in the subsurface, these tests were selected to investigate the responses of various Karoo rocks to the introduction of AMD. Moreover, the column leach tests allowed for a study of the interactions between the various rocks and the introduced AMD, reflecting their abilities to extract AMD pollutants, and allowing their buffering capacities to be ranked. Knowledge of the buffering capacities of the rocks can be used as an input to the regional modeling of transport and attenuation of AMD in coalfields to advise policy and decision makers. As an illustration of the concept, the Witbank, Ermelo and Highveld coalfields in the Mpumalanga Province of South Africa were selected. These coalfields are the most extensively exploited coalfields in the country and are the location of most current mining activities (Banks et al. 2011; Sakala et al. 2018).

STUDY SITE

Location and Climatic Conditions

The study area, which includes the Highveld, Ermelo and Witbank coalfields, is located in the Mpumalanga Province of South Africa, covering an area $\sim$ 23,315 km^2 (Fig. 1). The area receives an average long-term rainfall of between 600 and 1100 mm/a (SAWS 2016). The winters are typically dry and cold with occasional frost, while the summers, between October and March, are hot (Barnard 2000).

Geology and Hydrogeology

The local geological information used in this study was obtained from 1:250,000 scale geological maps (Pretoria 2528 and East Rand 2628) published by the Council for Geoscience (Fig. 1). The study area includes eight major lithological domains, namely the Basement Complex, the Witwatersrand Supergroup, the Transvaal Supergroup, the Bushveld Complex, the Dwarsfontein Complex, the Waterberg Group, the Karoo Supergroup and Tertiary–Quaternary alluvial deposits. The eight domains may further be resolved into 15 geological formations, including sedimentary, igneous and metamorphic rocks as well as lavas. According to Banks et al. (2011) and Sakala et al. (2018), many of the aquifer systems found within the Witbank, Ermelo and Highveld coalfields are shallow (between depths of 5 m and 20 m), a feature which makes them susceptible to pollution from mining operations. Hence, a study of how AMD chemically interacts with various rocks is required in these coalfields to delineate high-risk areas where AMD pollution is not attenuated and where it may therefore enter the groundwater system.

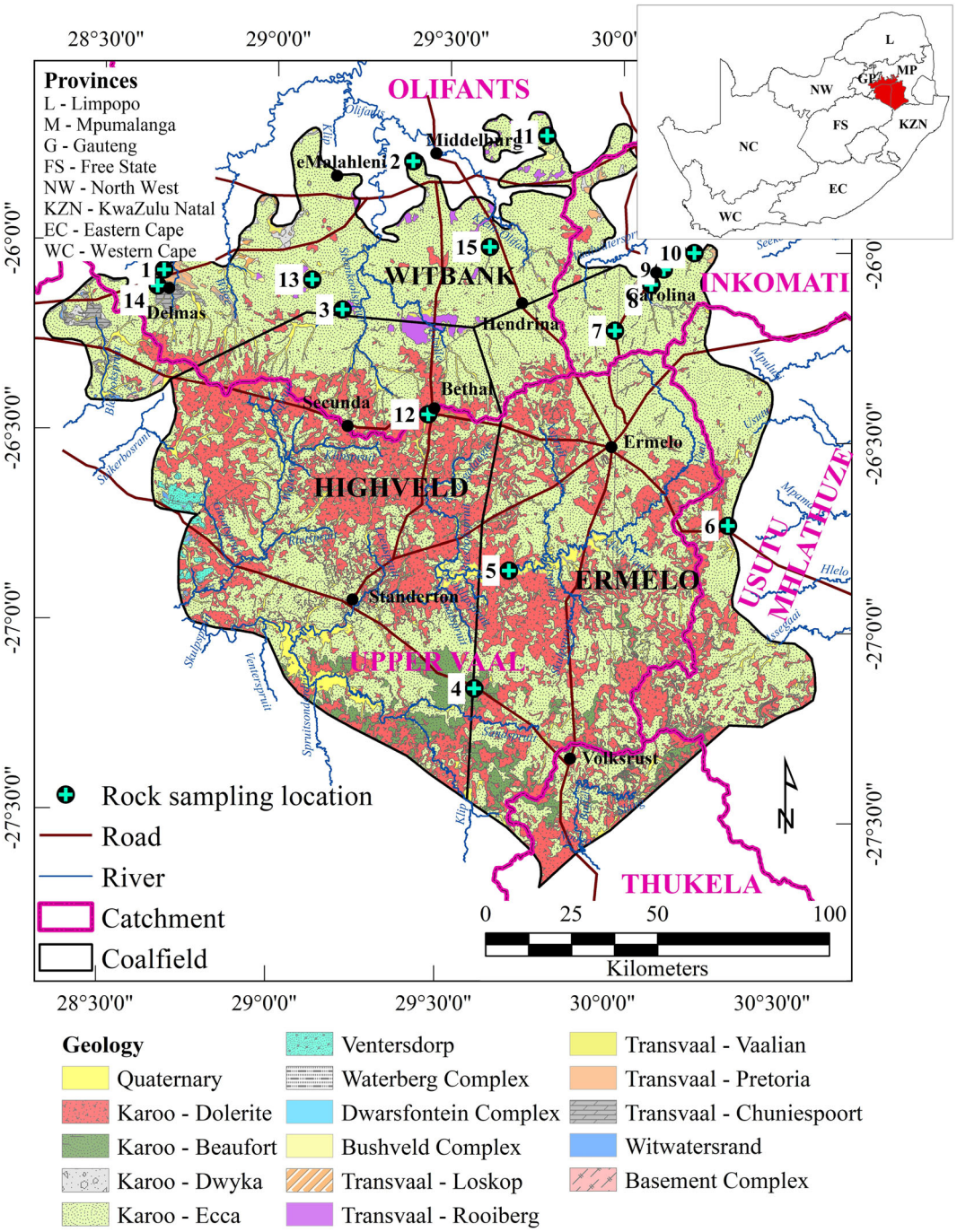

Figure 1. Geology of the study area. The inset map shows its location in South Africa.

METHODOLOGY

The column leach test, a kinetic testing procedure was conducted according to the United States Environmental Protection Agency (U.S Environmental Protection Agency 1994). In this column leach tests, AMD was used instead of de-ionized water as leachate to simulate the chemical interaction of AMD with various rock types rather than to characterize the rock samples in terms of their acid-

generating potential. The experimental procedure for the rock-AMD interaction study involved: (1) rock sample collection and analysis to identify mineralogical similarities across the various formations, (2) using representative samples for column leach tests under saturated and unsaturated conditions, and (3) analyzing the tests results, ultimately ranking rocks in terms of their effect on the removal of AMD pollutants as shown in Figure 2.

Sample Collection and Analysis

The study area includes 15 distinct geological formations, each mineralogically different from the others. Fresh grab samples were collected from all 15 formations where they have been exposed by mining within the study area. The locations of the 15 sampling positions are shown as black circles with green crosses in Figure 1. The fresh rock samples were analyzed for their elemental composition using X-ray fluorescence (XRF) and for mineralogy using X-ray diffraction (XRD) and using a microscope to aid in the interpretation of the column leach results and in view of understanding the general mineralogical distribution within the study area. Using the XRF and XRD results, the rock samples were sorted into groups according to their elemental compositions. AMD was collected from an abandoned underground mine in the Witbank coalfield.

Column Leach Tests

The saturated column and unsaturated column tests are set up as shown in Figure 3. For the saturated leach test (Fig. 3a), AMD was introduced from the bottom and passed through the rock sample to ensure its complete submersion in AMD. The unsaturated column test (Fig. 3b), AMD was fed occasionally from the open top and allowed to pass through the rock sample to allow reaction in the presence of air to mimic unsaturated conditions. The resultant leachate was analyzed weekly to collect enough data to allow a comparison between the leachates collected from the different samples. The parameters for the actual experiment were as follows: 45 cm column height and 11 cm column diameter, while the crushed rock added weighted 1.38 kg. The experiments were run until the oxidation reactions are completed. The flow rate for the saturated experiment was maintained at 0.01 ml/min to ensure that the column was completely saturated while at the same time allowing enough time for the reactions to occur. Leachate samples were collected on a weekly basis and analyzed by inductively coupled plasma-mass spectrometry (ICP-MS) and ion chromatography (IC).

RESULTS AND DISCUSSIONS

AMD was collected from a decanting abandoned underground mine in the Witbank coalfield. The chemical analysis of AMD is shown in Table 1. AMD that was collected has low pH with high concentrations of Fe, Al, Mn Zn and SO_4^{2-}. This means that the water was not suitable for discharge into the environment. The worst case scenario of AMD was used in this study.

Figure 4 shows the results of XRF and XRD analyses, plotted as a bar graph to facilitate visualization and comparison. Figure 4a shows that the most dominant elemental oxide for all the samples (except WITS14) is SiO_2 followed by Al_2O_3. Other elemental oxides that showed up prominently were MgO and CaO. These elemental oxides, which accounted for 10% or more of the composition of the samples, were found in samples WITS01, WITS09, WITS10, WITS11 and WITS14. The XRD results (Fig. 4b) show that sample WITS01 uniquely contained almost equal proportions of silicates, plagioclase, quartz and chlorite; thus, this sample was selected. Samples WITS07 and WITS14 were composed almost entirely of quartz and dolomite, respectively (Fig. 4b). These rocks are known to have almost opposite responses in an AMD environment (Eary and Williamson 2006). Using the XRF and XRD results, the 15 rock samples may be sorted into five groups according to their elemental compositions, as shown in Table 2.

The selected five representative samples (Table 2) were analyzed further under a microscope to establish in detail the spatial arrangement of their minerals and the results are shown in Figure 5. The sample section for diabase (WITS01) is dominated by medium- to coarse-grained elongated crystals of plagioclase feldspar with grain sizes in the order of 1.8 mm, with strongly colored varieties of augitic pyroxene (clinopyroxene characteristically) crystals wrapped around (Fig. 5a). The sample section of sandstone (WITS07) is dominated by medium- to fine-grained quartz, with some grains occurring as angular to sub-angular crystals, while others have

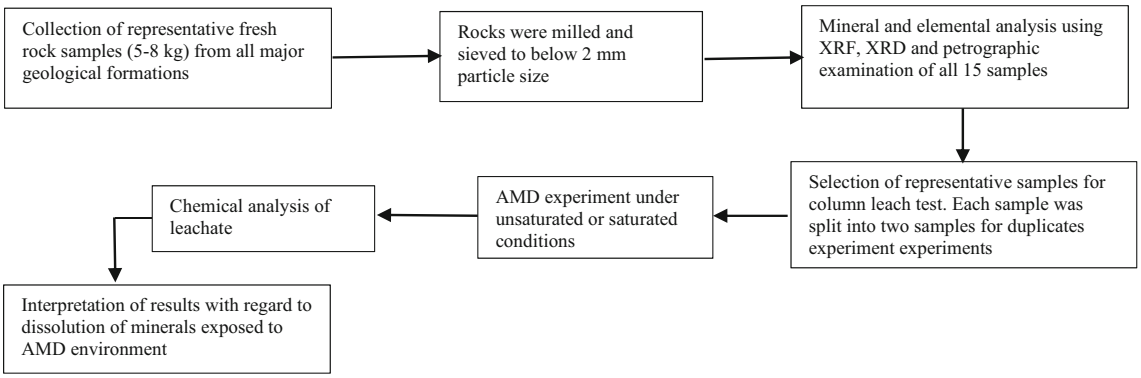

Figure 2. Methodology used in this study.

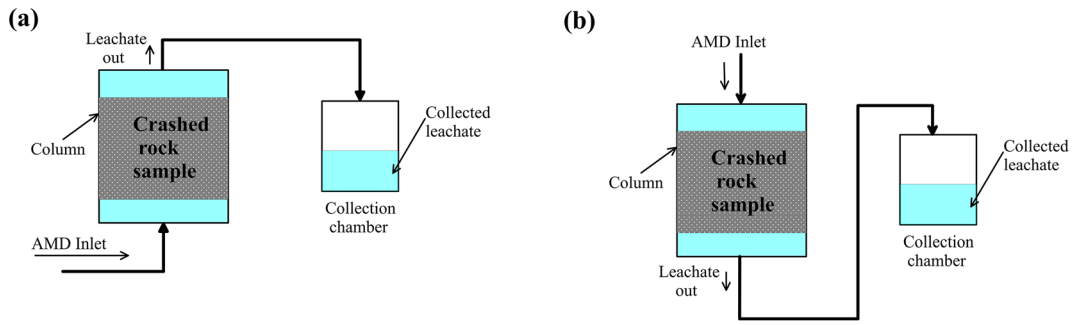

Figure 3. Schematic laboratory setup for column tests: (**a**) saturated; (**b**) unsaturated.

Table 1. Chemical composition of AMD used for column leach experiment

Parameter	Value
pH	2.2
EC (mS/cm)	806
Fe (mg/L)	1 815
Al (mg/L)	600
Mn (mg/L)	14.9
Zn (mg/L)	11.2
Cu (mg/L)	1.4
Co (mg/L)	3.4
Ni (mg/L)	4.6
As (mg/L)	0.1
Ag (mg/L)	0.00
Pb (mg/L)	0.00
SO_4^{2-} (mg/L)	7 045

euhedral grain size of ~ 0.68 mm (Fig. 5b). The pillow lava sample (WITS08) shows very fine-grained quartz minerals and feldspar crystals forming a clay-rich matrix around the sample (Fig. 5c). Feldspar occurs as fine-grained crystals, which makes it difficult to determine whether the section comprises plagioclase or sanidine, or both. Alteration phases observed in the section include chlorite, which occurs with clay minerals such as kaolinite. The hornfels sample (WITS09) is dominated by fine- to coarse-grained randomly oriented laths of plagioclase which generally exhibit lamella twinning (Fig. 5d). The plagioclase laths generally occur in localized clusters (grain size of < 3.15 mm) with interlocking grain-to-grain boundaries. The dolomite sample (WITS14) is dominated by fine-grained tightly packed anhedral crystals of calcite and dolomite (Fig. 5e). The dolomite crystals appear transparent, cloudy to dark in color. Calcite has high birefringence; its color with crossed polars shows distinctive rainbow colors of pink and green flashes. This section reveals dolomite and calcite presenting a mosaic of fine-grained crystals with poorly defined, non-planar boundaries.

The representative samples obtained (shown in Table 2), containing a proportion of silicates, plagioclase, quartz, clays, chlorite and dolomite minerals, were subjected to AMD experiments under saturated and unsaturated conditions.

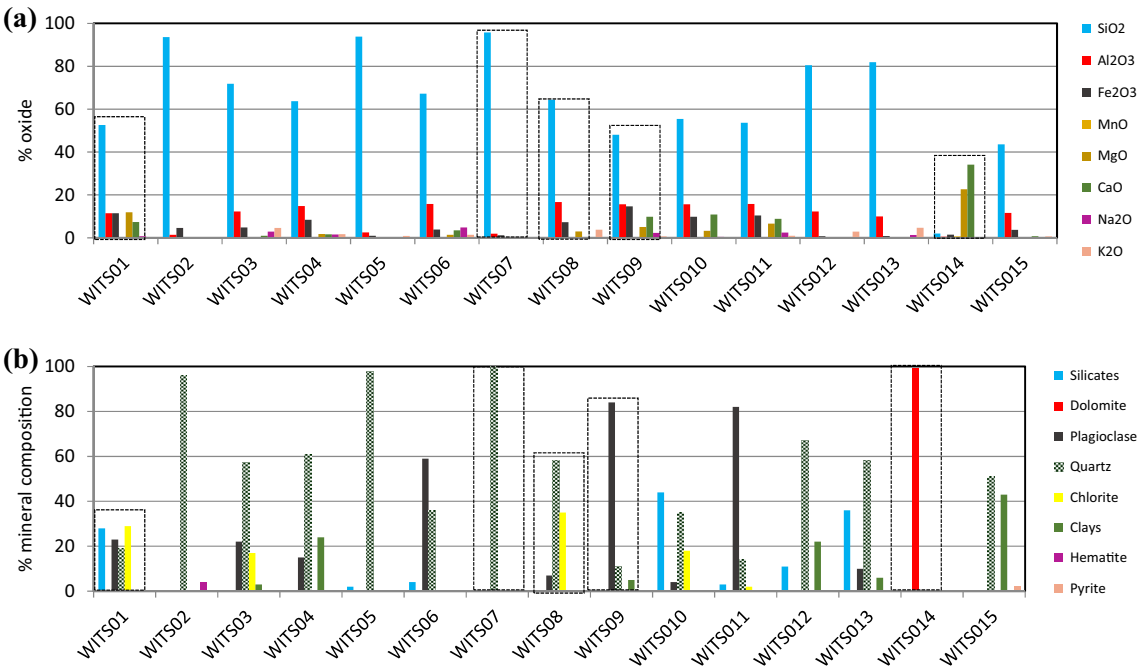

Figure 4. (**a**) Elemental compositions of rocks measured by XRF. (**b**) Mineral composition of the rocks determined by XRD, showing the five samples (enclosed in hallow rectangles) selected for the column leach experiment.

Table 2. Groups of samples according to their mineral speciation, as interpreted from XRF and XRD results

Sample name (WITss)	Major oxides	Major minerals identified	Group
01	SiO_2, Al_2O_3, Fe_2O_3, MgO, CaO, SiO_2	Equal proportions of silicates, plagioclase & quartz	I
02, 05, 07	SiO_2	Composed of entirely quartz	II
03, 04, 06, 08, 12, 13	SiO_2, Al_2O_3, Fe_2O_3	Made up of plagioclase < quartz < chlorite	III
09, 10, 11	SiO_2, Al_2O_3, Fe_2O_3, MgO, CaO	Made up of clays < quartz < plagioclase	IV
14	MgO, CaO	Composed entirely of dolomite	V

Silicate/Plagioclase/Quartz Sample (WITS01)

The leachate chemical analysis of sample WITS01 shows a minor change in the pH and electrical conductivity (EC) of the AMD in saturated conditions (Fig. 6a). Under unsaturated conditions, the pH changed from the AMD input of 2.8 to a near-neutral value ($\sim$ 7) from day 7 until day 29, when the neutralizing capacity was lost and the leachate pH returned to acidic conditions of around pH 4 (Fig. 6b). The order of magnitude of the concentrations of sulfate (SO_4^{2-}), manganese (Mn), aluminum (Al), calcium (Ca) and Cl did not change significantly under saturated conditions, reflecting the lack of their reactivity with AMD. A step increase in Na from 3 to 200 mg/L was observed. This may be explained by an ionic exchange reaction, where Mg ions from the AMD replaces Na ions from the rock matrix Eq. 1 (Casiday et al. 1999).

$$Z.Na + Y.Mg \leftrightarrow Z.Mg + Y.Na \quad (1)$$

where Z is the rock matrix and Y the AMD solution.

Fluctuations in the iron (Fe) concentration throughout the duration of the experiment could be a reflection of the instability of Fe under acidic conditions. At day 70, the concentration of magnesium (Mg) decreased at the same time that the concentration of sodium (Na) increased.

The order of magnitude of the EC and the concentrations of sulfate (SO_4^{2-}), Mn, Ca and Cl did not change significantly throughout the duration of

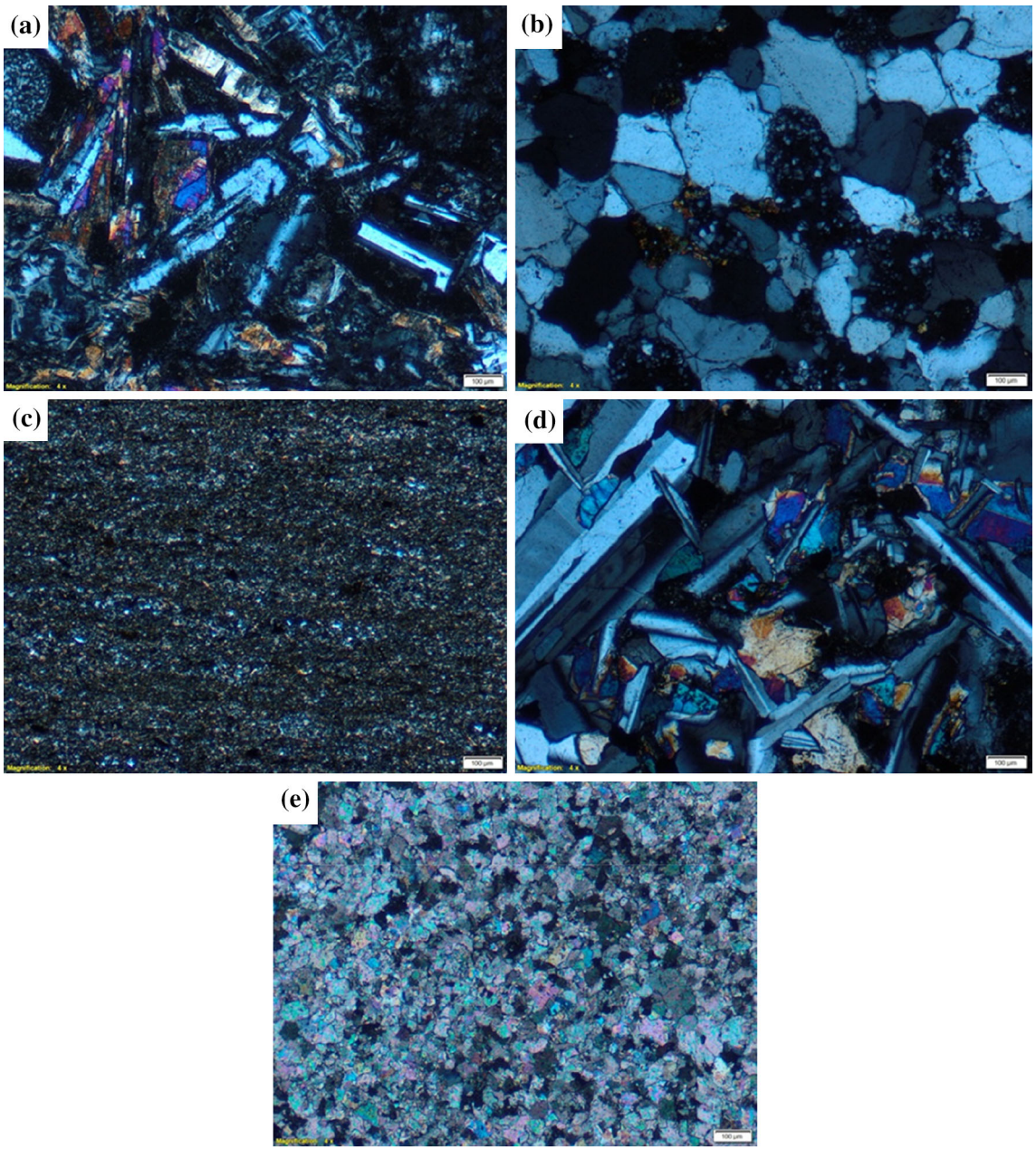

Figure 5. Images of rock sample thin sections, as observed on a Fein Optic R40POL polarizing microscope: (**a**) WITS01, (**b**) WITS07, (**c**) WITS08, (**d**) WITS09 and (**e**) WITS14.

the experiment in unsaturated conditions. The iron concentration decreased from 140 mg/L to values below 20 mg/L. The interchange between Mg ions and Na ions after day 70 was also observed under unsaturated conditions. When the pH was near-neutral, the concentration of Al drastically decreased to a concentration as low as 0.3 mg/L, but when the pH was acidic, the concentration of the leachate was similar to the Al concentration in the AMD solution. As the pH increased, hydrolysis made additional binding sites on the rock matrix available for Al complexation, and thus, aqueous Al was re-precipitated to form amorphous Al hydroxide, alumina-secondary minerals, Al–organic com-

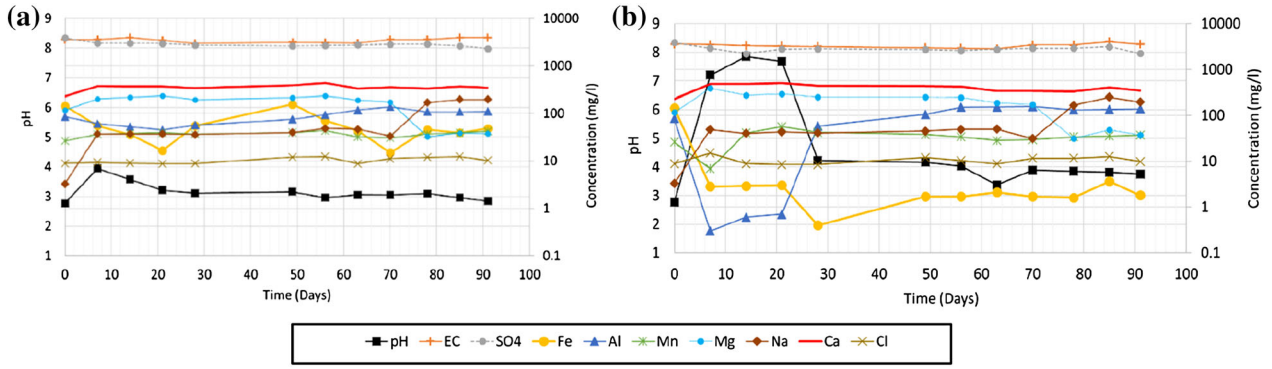

Figure 6. Graphic plot of leachate vs. time for WITS01: (**a**) saturated conditions; (**b**) unsaturated conditions.

plexes or large polymers, while the hydrogen ion produced in the process counteracted the effect of an increase in pH (Li and Johnson 2016). At low pH, Al complexes dissociated to offset the drop in pH, which increased their mobilization in solution.

Sample WITS01 is dominated by medium- to coarse-grained elongated crystals of plagioclase feldspar mostly made up of SiO_2, Al_2O_3, Fe_2O_3 and CaO elemental oxides, as shown by the XRF results. Thus, dissolution of anorthite ($CaAl_2Si_2O_8$) minerals under acid conditions can be used to explain the response of rocks containing plagioclase in an AMD environment. The dissolution of anorthite is a well-studied phenomenon, represented by Eq. 2, as given by Oelkers and Schott (1995):

$$CaAl_2Si_2O_8 + 8H^+ \leftrightarrow Ca^{+2} + 2Al^{+3} + 2SiO_2 + 4H_2O \quad (2)$$

According to Eq. 2, the dissolution of anorthite produces Ca^{+2} and Al^{+3} ions in solution. This phenomenon was particularly noted when the dissolution reactions took place for Sample WITS01, as evidenced by the change in pH from acidic to near-neutral accompanied by a slight increase in the Ca concentrations found in the leachate. However, no increase in Al^{+3} concentration was observed in the leachate, as the Al^{+3} ions immediately formed complexes of hydroxyl, which adhered to the grains of the rock matrix.

Quartz Sample (WITS07)

For both saturated and unsaturated conditions, the pH of the quartz sample remained fairly constant throughout the duration of the experiments (Fig. 7). The order of magnitude of the EC value and the concentrations of SO_4^{2-}, Mn, Ca, Al, Fe and Cl did not change significantly throughout the duration of the experiment. The interchange between Mg and Na observed for sample WITS07 was also evidenced after day 70 under both saturated and unsaturated conditions.

The dissolution of silicate minerals plays a bigger role in the response of sample WITS07 (made up of over 95% SiO_2) under an AMD environment. According to Kamiya et al. (1974), the dissolution of silicates is a very slow process, even in an acidic environment. This explains why no significant change was observed for the pH, SO_4^{2-}, Fe, Al and Mg concentrations of the WITS07 sample.

Plagioclase/Quartz/Chlorite Sample (WITS08)

The interchange between Mg and Na for samples WITS08 was also observed after day 70, for unsaturated as well as saturated conditions (Fig. 8). The initial slight increase in pH from 2.8 to 3.5 corresponded to a decrease in the Fe concentration from 145 to 5.8 mg/L under saturated conditions. When the pH regressed to 2.8 in the middle of the experiment, the Fe concentration correspondingly increased to 33 mg/L (Fig. 8a). The order of magnitude of concentration of EC, SO_4^{2-}, Mn, Al, Ca and Cl did not change significantly throughout the duration of the experiment.

Figure 8b shows that, under unsaturated conditions, the pH increased from 2.8 to 4.5 in the initial stages of the experiment and stabilized there for most of the experimental duration before regressing

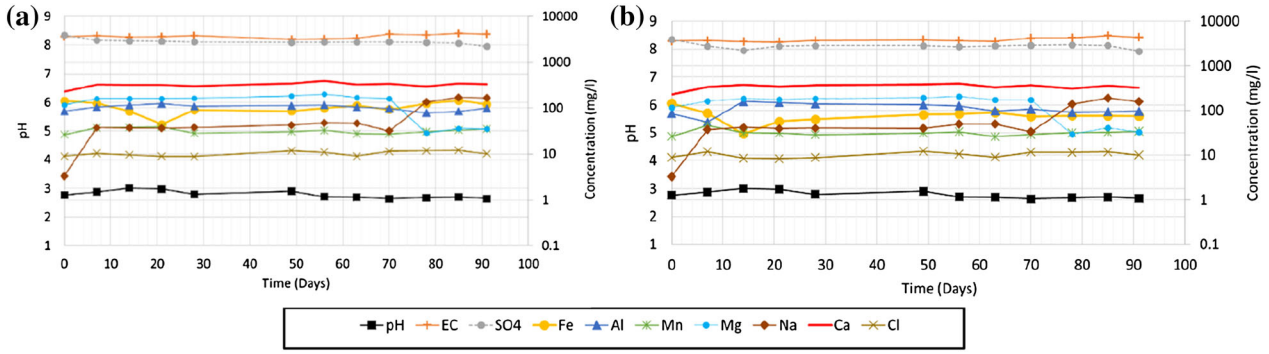

Figure 7. Graphic plot of leachate vs. time for WITS07: (**a**) saturated conditions; (**b**) unsaturated conditions.

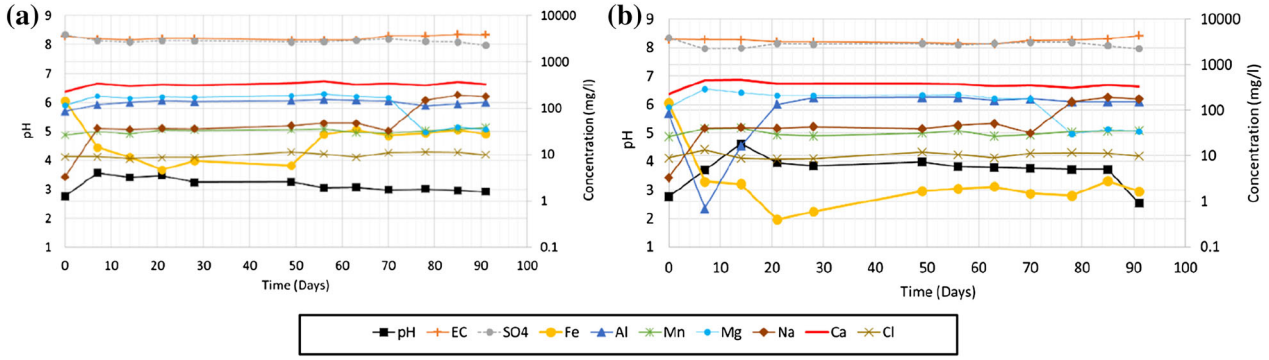

Figure 8. Graphic plot of leachate vs. time for WITS08: (**a**) saturated conditions; (**b**) unsaturated conditions.

to 2.8 at the end of the experiment. The order of magnitude of concentration of EC, SO_4^{2-}, Mn, Al, Ca and Cl did not change significantly throughout the experiment. A step increase in the concentration of Na from 3.7 to 177 mg/L was observed. When the pH increased to 4.5, the concentration of Al and Fe decreased from 85 and 145 mg/L to concentrations as low as 0.7 and 0.4 mg/L, respectively. Hydrolysis and the re-precipitation process, as discussed for WITS01, were responsible for the fluctuation in Al concentration as the pH changes (Li and Johnson 2016).

Sample WITS08 was made up of almost equal amounts of quartz minerals and plagioclase feldspar. Thus, a combination of the dissolution of plagioclase feldspar and the inertness of quartz (as already stated) could be used to explain the response observed for this sample. It must be noted that the resultant chemical concentration of the leachate from WITS08 was always between that of WITS7 and WITS9.

Clay/Quartz/Plagioclase Sample (WITS09)

In saturated conditions, the leachate chemical analysis shows that the pH increased slightly in the first few days before regressing to 2.8 (Fig. 9a). The concentration of Na and Mg followed similar trends for the duration of the experiment under saturated conditions. The concentration of Fe fluctuated between 50.4 and 185 mg/L throughout the experiment, as reflected by the unsteadiness of Fe under acidic conditions. The order of magnitude of concentration of SO_4^{2-}, Cl, Ca, Mn and Al did not change significantly throughout the duration of the experiment probably as also reflected by their lack of reactivity in acid conditions in saturated conditions.

In unsaturated conditions, the pH increased from the AMD input value of 2.8 to a near-neutral value $\sim$ 7 after the first few days of the experiment after which the neutralizing capacity was lost and the leachate pH returned to acidic conditions of around

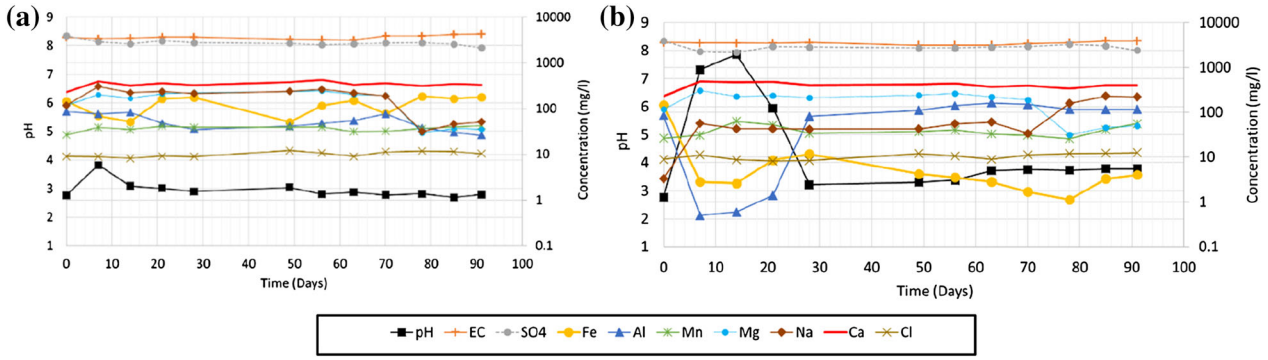

Figure 9. Graphic plot of leachate vs. time for WITS09: (**a**) saturated conditions; (**b**) unsaturated conditions.

pH 3.5 (Fig. 9b). The interchange between Mg and Na toward the end of the experiment was also observed in unsaturated conditions. The order of magnitude of concentration of EC, SO_4^{2-}, Cl and Ca also did not change significantly throughout the duration of the experiment. When the pH increased to near-neutral, the concentration of Al and Fe decreased from 85 and 145 mg/L to concentrations as low as 0.5 and 1.1 mg/L, respectively, owing to the formation of hydroxides at pH above 4.

Dolomite Sample (WITS14)

Both for saturated and unsaturated conditions, the pH of the leachate for sample WITS14 buffered the acidity from 2.8 to a pH of around 8 from the first few days of the experiment until the end (Fig. 10a, b). This was attributable to the dissolution of dolomite in an acid environment, as given by Eq. 3 and as stated by Stumm and Morgan (1996) and Gomo and Masemola (2016).

$$CaMg(CO_3)_2 + 4H^+ \leftrightarrow Ca^{+2} + Mg^{+2} + 2H_2O + 2CO_2 \quad (3)$$

Minor changes in the EC, SO_4^{2-}, Cl and Mn of the leachate under saturated conditions were observed for the dolomite sample. A stepward increase in Na from 3.2 to 321 mg/L was also observed. Similar to the saturated conditions, the order of magnitude of concentration of EC, SO_4^{2-}, and Cl did not change significantly throughout the duration of the experiment, probably reflecting the lack of their participation in reactivity under these conditions.

In both the saturated and the unsaturated conditions, when the pH increased to near-neutral, the concentration of Al and Fe decreased from 85 and 145 mg/L to concentrations as low as 0.1 and 0.9 mg/L, respectively. This could be ascribed to the precipitation of hydroxides as the pH increased to near-neutral. The concentration of Mn decreased from 26 to 0.3 mg/L in the first two weeks and then increased gradually back to 26 mg/L toward the end of the experiment.

In the column with sample WITS14, dolomite is the major carbonate available to neutralize the pH. The dolomite-AMD buffering reaction (Eq. 3) conceptually shows that when the acid, H^+ from the AMD reacted with dolomite ($CaMg(CO_3)_2$); water (H_2O), carbon dioxide (CO_2), calcium (Ca^{+2}) and magnesium (Mg^{+2}) are produced. Based on this conceptual model, when such reactions occur, Ca and Mg concentrations are likely to be increased. This was indeed the case for WITS14, as seen in the Ca and Mg plots under unsaturated conditions where both oxygen and water were present. At the same time, Fe concentrations decreased as free Fe ions formed complexes adhering to the mineral grains of the rock sample, thus accounting for the observed decreased Fe concentration. The solubility of Al and Mn is pH dependent (Wright et al. 2001) when pH was neutral they precipitated and when pH was low they were in solution.

Ranking of Geological Formations in Terms of AMD Extraction

Based on the interpretation of the leachate concentration in relation to the rock mineral com-

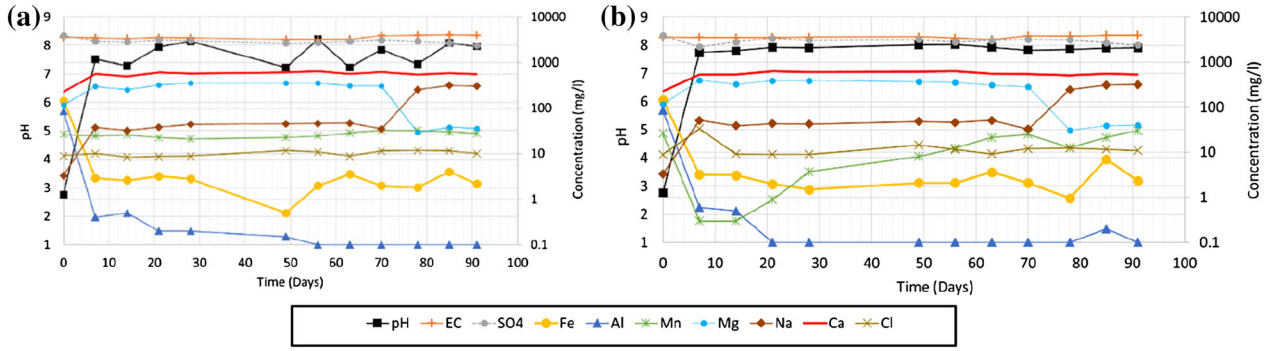

Figure 10. Graphic plot of leachate vs. time for WITS14: (**a**) saturated conditions; (**b**) unsaturated conditions.

position for various rocks in the AMD environment, an approximate order of rock-AMD reactivity can be deduced for the Witbank, Ermelo and Highveld coalfields. Table 3 shows a summary of the findings of the experiment.

From the experiment, it can be deduced that dolomite, which contains over 90% dolomitic carbonate minerals, was able to buffer the pH to neutral conditions which, in turn, removed the metals (Fe, Al and Mn) from the AMD solution. Diabase with medium- to coarse-grained elongate crystals of plagioclase feldspar which are Al complexes was also able to buffer the acidic conditions, but given that the buffering minerals are easily exhausted, buffering only lasted a few weeks.

In terms of AMD extraction by rocks, hornfels followed diabase where the fine- to coarse-grained randomly oriented laths of plagioclase are responsive in buffering the acidic conditions and removing heavy minerals. The process is kinetically fast and only lasted a few weeks. Pillow lava, which is dominated by very fine-grained quartz and feldspar crystals, was also able to buffer the acidity to a lesser extent, but the process lasted a few days. Sandstones were the least effective in terms of buffering acidity and removing heavy metals (Fe, Al and Mn) from AMD solution. The sandstones are made up almost entirely of quartz minerals which lack the ability to buffer acidity or remove heavy metals in the time frame of the experiment.

Hardly any rocks tested were able to remove sulfates and chlorides under saturated and/or unsaturated conditions. Moreover, all the rock leachates were shown to follow an almost similar pattern over time. Thus, sulfate and chlorides may be considered conservative in both saturated and unsaturated conditions and can be used as a possible tracer for AMD pollution. Another interesting observation from the experiment is that pH buffering and metal removals were more pronounced in the unsaturated zone than in the saturated zone as a result of the presence of oxygen.

The results from the rock-AMD reactivity experiment can be used as a guide to the classification of the rocks in the coalfields based on the mineralogical similarities between those rocks and the rock samples used in the experiment.

Table 4 shows the classification of various rocks found in Witbank, Ermelo and Highveld coalfields in terms of their reactivity in the AMD environment.

The rocks were assigned relative values from 1 to 10 according to their ability to buffer acidity and remove heavy metal pollutants typically associated with AMD pollution in the Witbank, Ermelo and Highveld coalfields. Figure 11 shows the spatial distribution classes of rock-AMD reactivity within these coalfields as resampled to the geological formations, using the results of the experiment. The distribution of surface geologies for which different AMD reactivity was determined during this study and deeper geologies were not considered. The map in Figure 11 was therefore only a first indication of the distribution of AMD reactivity and not a comprehensive mapping of AMD reactivity in the study area.

CONCLUSIONS AND RECOMMENDATIONS

From the results obtained, the following conclusions were reached. The quartz sample was unreactive to AMD in both saturated and unsatu-

Table 3. Summary of rock-AMD reactivity expressed in terms of AMD removal by rocks

Parameter	Order of AMD reduction by rocks	Remarks
pH	WITS 14 > WITS 1 > WITS 9 > WITS 8 > WITS 7	Dolomite buffered acidity better than other rocks and sandstone being the least
EC	WITS 1 > WITS 8 > WITS 9 > WITS 14 > WITS 7	Diabase/dolerite rocks reduced the EC better than most rocks with sandstone being the least in this regards
SO_4	WITS 1 = WITS 7 = WITS 8 = WITS 9 > WITS 14	Sulfate generally remained unaffected by interaction with various rocks
Fe	WITS 14 > WITS 1 = WITS 8 > WITS 9 > WITS 7	Dolomite removed Fe better than other rocks and sandstone being the least
Al	WITS 14 > WITS 1 > WITS 9 > WITS 8 > WITS 7	Dolomite removed Al better than other rocks and sandstone being the least
Mn	WITS 14 > WITS 1 > WITS 9 > WITS 8 > WITS 7	Dolomite removed Mn better than other rocks and sandstone being the least

WITS 14 Dolomite, *WITS 1* Diabase, *WITS 9* Hornfels, *WITS 8* Pillow lava, *WITS 7* Sandstone

Table 4. Summary of AMD reactivity of rocks in the Witbank, Ermelo and Highveld coalfields

Lithological group	Description	Sample representative	Relative reactivity (1–10)
Quaternary			
Alluvial	Unconsolidated sediments on rivers	WITS 7	1
The Karoo supergroup			
Dwyka group	Diamictite (Tillite)	WITS 7	1
Ecca group	Sandstone, shale and coal	WITS 7	1
Beaufort group	Mudrock, sandstone	WITS 1	7
Intrusive rocks	Dolerite (dykes and sills)	WITS 1	7
Waterberg complex	Sandstone with interbedded conglomerate and shale	WITS 7	1
The bushveld complex			
Rustenburg suite	Gabbro, norite, anorthosite	WITS 9	5
Lebowa suite	Felsic granite	WITS 9	5
Transvaal supergroup			
Chuniespoort group	Dolomite, chert	WITS 14	9
Pretoria group	Shale, quartzite	WITS 1	7
Intrusive rocks	Diabase	WITS 1	7
Rooiberg group	Rhyolite and felsite	WITS 8	3
Loskop formation	Sandstone, conglomerate	WITS 7	1
Witwatersrand supergroup			
Hospital hill formation	Shale and quartzite	WITS 1	7
Basement complex	Granite and gneiss	WITS 9	5

rated conditions within the duration of the experiment. This means that, if AMD is generated from mine tailings in an environment comprising mainly quartz, there will be pollution of the water resources by AMD. On the other extreme, dolomite was capable of neutralizing AMD under both conditions. In other words, AMD generated by mine tailings on dolomite will result in in situ neutralization of acidity and reduction in pollution of water resources by AMD. An increase in pH will result in the precipitation of metals as hydroxides. In addition, coprecipitation of minor elements in AMD will occur during the precipitation of hydroxides such as $Fe(OH)_3$. The performance of plagioclase minerals was also affected by these conditions. In saturated conditions (that is, O_2 depleted conditions), the plagioclase minerals did not neutralize AMD. On the other hand, in unsaturated conditions (in the presence of O_2), AMD was neutralized. Therefore, it can be concluded that the presence of O_2 enhanced the dissolution of plagioclase minerals. Clay minerals are known to possess ion exchange capabilities. The presence of clay minerals enhanced the neutralization of acidity and the removal of cations from AMD. Therefore, AMD generated by mine tailings can be contained by subsurface with dolo-

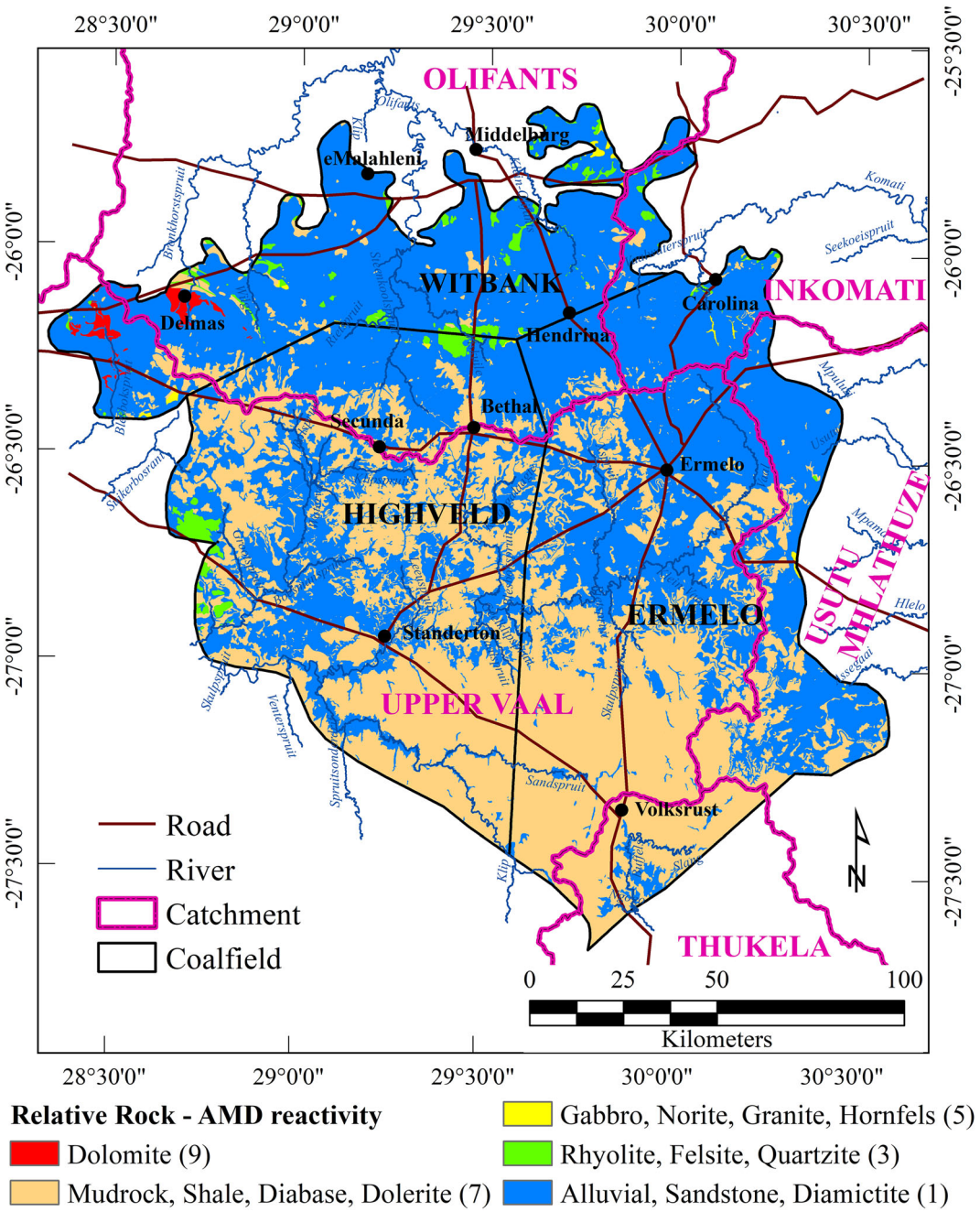

Figure 11. Rock-AMD reactivity map of the study area showing the relative classifications in terms of the extraction of AMD pollutants.

mite, plagioclase and/or clay minerals as these minerals will provide natural attenuation of the pH and some of the potential pollutants.

The column leach tests were conducted at room temperature, with reduced particle size and without seasonal variations and extremes of precipitation. Consequently, they provide poor analogues for heterogeneous drainage conditions and secondary mineral precipitation and dissolution, the controlling factors for metal leaching under all but the most

acidic pH values. Given the absence of the entire load of primary weathering products, leachate results cannot be used with geochemical speciation models to predict the extent of secondary precipitation or release, or with field data to predict metal leaching based on the predicted evolution in drainage chemistry (i.e., pH conditions). For further researches, these conditions could be incorporated to refine the interpretations made here to cover changing environmental conditions.

ACKNOWLEDGMENTS

The authors would like to thank the Department of Mineral Resources and the Council for Geoscience the research funding and access to the various datasets used in this study.

REFERENCES

Banks, V. J., Palumbo-Roe, Van Tonder, D. B., Davies, J., Fleming, C., & Chevrel, S. (2011). Conceptual models of the Witbank coalfield, South Africa. Earth observation for monitoring and observing environmental and societal impacts of mineral resources exploration and exploitation, CEC FP7 Project EO-MINERS, Deliverable D3.

Barnard, H. C. (2000). An explanation of the 1:500,000 general hydrogeological map-Johannesburg, 2526.

Bell, F. G., Hälbich, T. F. J., & Bullock, S. E. T. (2002). The effects of acid mine drainage from an old mine in the Witbank Coalfield. *South Africa, Quarterly Journal of Engineering Geology & Hydrogeology, 35,* 265–278.

Casiday, R., Noelken, G., & Frey, R. (1999). Treating the public water supply: What is in your water, and how is it made safe to drink? Inorganic Reactions Experiment [WWW Document]. Washington University. Retrieved August 23, 2018 from http://www.chemistry.wustl.edu/~edudev/LabTutorials/Water/PublicWaterSupply/PublicWaterSupply.html.

Costin, D., Baciu, C., Pop, C., & Varga, I. (2011). Field-based kinetic testing of ARD potential of the waste rock from Ros ia montană ore deposit (Apuseni mountains, Romania). In R. Freund & A. Wolkersdorfer (Eds.), *13th IMWA mine water: Managing the challenges* (pp. 677–682). Aachen: IMWA.

De Souza, C. M. B., & Mansur, M. B. (2011). Modelling of acid mine drainage (AMD) in columns. *Brazilian Journal of Chemical Engineering, 28,* 425–432.

Eary, E. L., & Williamson, M. A. (2006). Simulations of the neutralising capacity of Silicate rocks in acid mine drainage environments. In *7th international conference on acid rock drainage (ICARD)*.

Gautama, R. S., & Kusuma, G. J. (2008). Evaluation of geochemical tests in predicting acid mine drainage potential in coal surface mine. In *10th international mine water conference* (pp. 271–274).

Gomo, M., & Masemola, E. (2016). Groundwater hydrogeochemical characteristics in rehabilitated coalmine spoils. *Journal of African Earth Science, 116,* 114–126.

Hadžić, E., Lazović, N., & Mulaomerović-Šeta, A. (2015). The importance of groundwater vulnerability maps in the protection of groundwater sources. *Key Study: Sarajevsko Polje, Procedia Environmental Science., 25,* 104–111.

Kamiya, H., Ozaki, A., & Imahashi, M. (1974). Dissolution rate of powdered quartz in acid solution. *Geochemical Journal, 8,* 21–26.

Lapakko, K. (2002). Metal mine rock and waste characterization tools: An overview. *International Institute for Environment and Development., 67,* 1–30.

Li, W., & Johnson, C. E. (2016). Relationships among pH, aluminum solubility and aluminum complexation with organic matter in acid forest soils of the Northeastern United States. *Geoderma, 271,* 234–242.

Oelkers, E. H., & Schott, J. (1995). Experimental study of anorthite dissolution and the relative mechanism of feldspar hydrolysis. *Geochimica et Cosmochimica Acta, 59,* 5039–5053.

Sakala, E., Fourie, F., Gomo, M., & Coetzee, H. (2017). Mapping surface sources of acid mine drainage using remote sensing: Case study of the Witbank, Ermelo and Highveld coalfields. In C. Wolkersdorfer, L. Sartz, M. Sillanpää, & A. Häkkinen (Eds.), *13th international mine water association congress: Mine water & circular economy* (pp. 1246–1253). Lappeenranta: IMWA.

Sakala, E., Fourie, F., Gomo, M., & Coetzee, H. (2018). GIS-based groundwater vulnerability modelling: A case study of the Witbank, Ermelo and Highveld Coalfields in South Africa. *Journal of African Earth Science, 137,* 46–60.

South African Weather Service (SAWS). (2016). Historical rain maps. Retrieved March 23, 2016, from http://www.weathersa.co.za/climate/historical-rain-maps.

Stumm, W., & Morgan, J. J. (1996). *Aquatic chemistry: Chemical equilibria and rates in natural waters* (3rd ed.). New York: Wiley.

U.S Environmental Protection Agency. (1994). Acid mine drainage prediction, EPA530-R-94-036.

Usher, B. H., Cruywagen, L. M., de Necker, E., & Hodgson, F. D. I. (2003). On-site and laboratory investigations of spoil in opencast collieries and the development of acid-base accounting procedures. WRC Report No. 1055/1/03.

Wright, W. G., Simon, W., Bove, D. J., Mast, M. M., & Leib, K. J. (2001). Distribution of pH values and dissolved trace-metal concentrations in streams. In: Church, S. E., von Guerard, P., & Finger, S. E. (Eds.), *Integrated investigations of environmental effects of historical mining in the Animas River Watershed, San Juan County, Colorado. U.S. Geological Survey* (pp. 501–539).